Nucleation Mode Formation in Heavy-Duty Diesel Exhaust with and without a Particulate Filter

ARTICLE *in* ENVIRONMENTAL SCIENCE AND TECHNOLOGY · OCTOBER 2004

Impact Factor: 5.33 · DOI: 10.1021/es0353255 · Source: PubMed

4 AUTHORS, INCLUDING:

Annele Virtanen
University of Eastern Finland
88 PUBLICATIONS **1,772** CITATIONS
SEE PROFILE

Jorma Keskinen
Tampere University of Technology
190 PUBLICATIONS **2,967** CITATIONS
SEE PROFILE

Environ. Sci. Technol. **2004**, *38,* 4884−4890

Nucleation Mode Formation in Heavy-Duty Diesel Exhaust with and without a Particulate Filter

KATI VAARASLAHTI, ANNELE VIRTANEN, JYRKI RISTIMÄKI, AND JORMA KESKINEN*

Institute of Physics, Aerosol Physics Laboratory, Tampere University of Technology, P.O. Box 692, FIN-33101 Tampere, Finland

Particle size distribution measurement with direct tailpipe sampling is employed to study the effect of a continuously regenerating diesel particulate filter (CRDPF) on emissions of a heavy-duty diesel engine. The CRDPF consists of an oxidation catalyst and a filter. Tests are conducted using 2 and 40 ppm sulfur content fuels and two steady-state driving modes. The formation of nucleation mode with and without CRDPF is found to depend on different parameters. Without after-treatment, size distribution is observed to have a nucleation mode only at low load. Being independent of the fuel sulfur level (with these low sulfur level fuels), this nucleation mode is suggested to form mainly from hydrocarbons. With a CRDPF-equipped engine, nucleation mode, which was not observed without CRDPF, was found at high load mode only. This nucleation mode formation was found to correlate positively with fuel sulfur content. It is suggested that sulfuric acid is a main nucleating species in this situation, resulting from the effective conversion of SO_2 to SO_3 in the oxidation catalyst. Using a thermodenuder confirms that the nucleation mode particles are semivolatile in nature.

Introduction

Diesel exhaust particles constitute an environmental and health hazard. Through the development of engine and after-treatment technologies, the mass concentration of these particles has been significantly reduced over the last years. At the same time, the interest in the particle number concentration and size distribution has increased. The submicron size distribution of diesel exhaust typically constitutes of two modes, often named as the accumulation and nucleation modes (*1*). Most of the particle mass is in the accumulation mode. The accumulation mode particles are solid carbonaceous agglomerates formed in the engine through incomplete combustion of fuel hydrocarbons. The gas cools in the exhaust line and in the dilution process when the exhaust is emitted, resulting in adsorption and possibly even condensation of semivolatile components on the accumulation mode particles. The nucleation mode particles consist of semivolatile organic and sulfur compounds. The compounds nucleate during the exhaust dilution processes as the gas exits the tailpipe to form liquid nanoparticles typically smaller than 50 nm in diameter. Only 1−20% of the particle mass is in the nucleation mode, but it may contribute to even more than 90% of the particle number. In addition to diesel exhaust in laboratory tests, these nanoparticles are also found in the urban atmosphere (e.g., refs *2* and *3*).

Exhaust filters called traps or diesel particulate filters (DPF) can be used to reduce diesel particulate emissions. Many types of filters with different regeneration systems and different types of filtration systems are nowadays available. A wall-flow monolith is the most common type of filtration element, where alternatively plugged channels force the diesel exhaust through porous walls and trap the particulate matter. Regeneration of the filter may be accomplished either with an active or a passive system. Electric regeneration and fuel burners are examples of active regeneration. Passive regeneration is done with the aid of catalysts, either placed directly onto the filter surface or added to the diesel fuel as fuel additive. A separate catalyst may also be placed upstream of the filter to generate nitrogen dioxide, which then oxidizes the soot collected in the filter. The filters are typically very effective at removing the solid particles, with measured efficiencies better than 99% (*4*, *5*). The collection efficiency for nucleation mode particles is not unambiguous, and the filters have been found to enhance the formation of the nucleation mode (*4*, *6*−*8*).

In this paper the formation of nucleation mode particles is studied during dilution of a heavy-duty diesel engine exhaust. The study is done with one engine, with two different fuels in different dilution conditions. All combinations were measured both without after-treatment and with an oxidation catalyst−filter combination installed.

Formation of Nanoparticles

Diesel particle emissions depend on many factors, such as the engine, after-treatment, fuel, lubricating oil, and driving conditions, which make the comparison of results of diesel exhaust studies often difficult. However general trends can be found and applied also to this study. The purpose of this section is to present the important trends, from this paper's point of view, from the past studies on the formation of nanoparticles (diameters below 50 nm) in diesel exhaust.

Nanoparticle formation during dilution processes has been reported in several studies (e.g., refs *6* and *9*). These nanosized particles do not have a solid core, but they are semivolatile and have been found to evaporate completely when heated to 175 °C (*10*). Their formation through nucleation is sensitive to the dilution ratio and temperature of the dilution during the dilution process (e.g., ref *11*).

There is limited understanding of the formation process of nanoparticles in exhaust gas dilution. A number of species are known to be able to nucleate under environmental conditions. Nucleation of sulfuric acid with water is the best known process and has been proposed as a main cause (*9*). Almost all sulfur in diesel exhaust is oxidized into SO_2 during combustion, but a small fraction is converted to SO_3 leading to formation of H_2SO_4 vapor. Depending on the dilution ratio and temperature, the vapor may then nucleate to form particles. Some calculations suggest that the predicted binary H_2SO_4−H_2O nucleation rate be in the right range to form significant number concentrations during exhaust dilution (*9*). Later, Vehkamäki et al. (*12*) extended the parametrization for binary H_2SO_4−H_2O nucleation model up to temperatures 300−400 K. However, calculations still do not give an outright agreement with the measurement results concerning real exhaust gas size distributions. Other components, mainly hydrocarbons, are also proposed (*6*, *13*). This is supported by the fact that nucleation mode has been detected also when the fuel sulfur content is very low (*8*, *14*). Hydrocarbons

* Corresbonding author phone: +358 3 3115 2676; fax: +358 3 3115 2600; e-mail: jorma.keskinen@tut.fi.

have been found to be the dominant species in nucleation mode particles also with fairly high sulfur content (400 ppm) fuels (*15*). The results from Tobias et al. (*15*) indicate that nanoparticle formation involves homogeneous binary nucleation of sulfuric acid and water followed by growth from condensation of organic species. Yu (*16*, *17*) has proposed ion induced nucleation caused by engine emitted chemiions as a possible process. Notwithstanding the nucleating species, the occurrence of the nucleation phenomenon has been suggested to be associated with lowered condensation sink of the accumulation mode for low soot emitters (*1*, *6*, *18*).

When after-treatment equipment, either filter or catalyst or both, is used, enhanced nucleation mode formation has been detected in many studies (e.g., refs *6*−*8* and *19*−*24*). The low carbon emissions downstream of filter have been suggested to favor nucleation through decreased adsorption of particle precursors onto accumulation mode particles (*6*−*8*). This nucleation mode is observed usually at high engine loads. Liu et al. (*7*) has suggested the higher formation rate of sulfur and organic compounds in the engine as the reason (*7*). A subsequent study indicates that the sulfur is the main nucleating component, as no nucleation mode was observed with using a low level sulfur fuel (*20*). When oxidation catalyst or catalyzed filter is used, the catalyzed reaction of sulfur dioxide to sulfur trioxide is proposed to favor the nucleation mode formation (*21*−*24*). High temperatures inside the after-treatment system favoring this reaction are reached at higher load driving modes. This suggestion is also supported by the result of chemical analysis of filter samples, which reveals an increase of the sulfate content (*21*). Most of the studies suggesting the nucleation mode formation downstream of a filter or a catalyst is related to SO_3 formation are done with rather high fuel sulfur levels (hundreds of ppm) (*7*, *20*−*23*). However, Kittelson et al. (*24*) also found a nucleation mode downstream of a catalyzed filter at much lower fuel sulfur level (26 ppm). A nucleation mode has also been detected during the regeneration phase of the filter and has been attributed to desorption of hydrocarbons caused by increasing temperature (*19*).

Many studies have documented the occurrence of traffic related ultrafine particles in urban areas (*2*, *3*, *25*, *26*) and in road tunnels (*27*, *28*). That these particles indeed form through nucleation during the dilution of fresh vehicle exhaust has been verified with chase experiments (*23*, *24*). It is impractical to try to completely mimic all atmospheric dilution conditions in laboratory studies. However, laboratory dilution systems should be able to reproduce the trends caused by changes in engine and after-treatment technologies, fuels, and lubricants. Until now, only the first steps have been taken in studying how nucleation is reproduced in laboratory control experiments on chassis dynamometer (*29*).

Experimental Section

Engine, Fuels, Filter, and Driving Modes. Measurements were done using a heavy-duty diesel engine Volvo DH 10A-285, a 1996 model year that meets Euro II emission standards. More details about this engine are presented in Table 1.

Two different fuels were used to study the effect of fuel sulfur level, an ultralow sulfur level fuel (2 ppm) and low sulfur level fuel (40 ppm) (Table 2). The lubricating oil was a commercial Neste Turbo LXE, and it was used in all measurements.

Measurements were done with no aftertreatment at all and with a filter installed on the place of a muffler (Figure 1). The filter was a continuously regenerating diesel particulate filter known as CRDPF or CRT (trademark of Johnson-Matthey). Later, it is s referred to as CRDPF in this paper. The regeneration of this filter is based on the finding that NO_2 oxidizes soot in lower temperatures than oxygen. The needed NO_2 is made in an oxidation catalyst installed upstream of the filter from the NO in exhaust gas (*30*). In CRDPF, the particulate filter itself is an uncatalyzed cordierite wall-flow honeycomb with cell density of 100 cpsi. The CRDPF system was sized for the engine used in these measurements. The filter back pressure was followed throughout the measurements to ensure that it did not exceed the limit value given by the manufacturer. No additional help for regeneration of the filter was used during the tests. Temperatures before (BCRDPF) and after (ACRDPF) CRDPF were measured as close to the CRDPF as it was possible. When there was no filter installed on the exhaust line the temperatures were measured before and after a muffler, which was in the same place as the filter.

TABLE 1. Engine Specification

engine	Volvo DH 10A-285
model year	1996
emission standards	EURO 2
cylinders	6 inline
displacement	9.6 L
fuel system	electronically controlled
configuration	turbocharged
peak power	210 kW at 2000 rpm
peak torque	1200 Nm at 1450 rpm
compression ratio	20:1

TABLE 2. Fuel Specification

		ultralow sulfur level	low sulfur level		
sulfur	Antek	2	40	mg/kg	ASTM D 5453
density	+15 °C	831.9	842.6	kg/m^3	ISO 12185
distillation	5% (vol)	200.1	212.1	°C	ISO 3405
	95% (vol)	345.0	356.2	°C	ISO 3405

For each configuration, measurements were made at two steady-state conditions, corresponding to modes 10 and 11 of the European steady cycle (ESC). The modes have same speed but different load, as shown in Table 3.

Aerosol Sampling and Measurement System. To study nucleation mode, a sampling and dilution system is needed that is repeatable and well-characterized. We use a modified version of the partial flow sampling system (PFSS) developed for the "Particulates" research program of EU. As described by Ntziachristos et al. (*29*), the basic idea is to dilute the exhaust gas immediately at exhaust pipe end with a porous tube type primary diluter. The primary diluter is described in detail by Mikkanen et al. (*31*). With PFSS, conditioning of the exhaust aerosol can be performed in the same manner regardless of the physical environment where the measurement is conducted. According to Ntziachristos et al. (*29*), comparison of PFSS measurements with size distributions obtained by chasing experiments demonstrate that the sampling system developed is able to accurately reproduce the accumulation mode and the potential for nucleation mode formation.

The original PFSS system was modified by placing the primary diluter outside the exhaust pipe and sampling through a 10 cm long metal tube. Another modification is that the entire sample passes through a secondary dilution unit. These modifications make the system easier to operate for our limited scope but are not expected to change sampling efficiency or dilution characteristics. Figure 1 shows a schematic diagram of the system.

Values of 12 and 25 were used for primary dilution ratio, which was adjusted by changing the exhaust gas flow rate with a mass flow controlled (MFC) bypass pump before

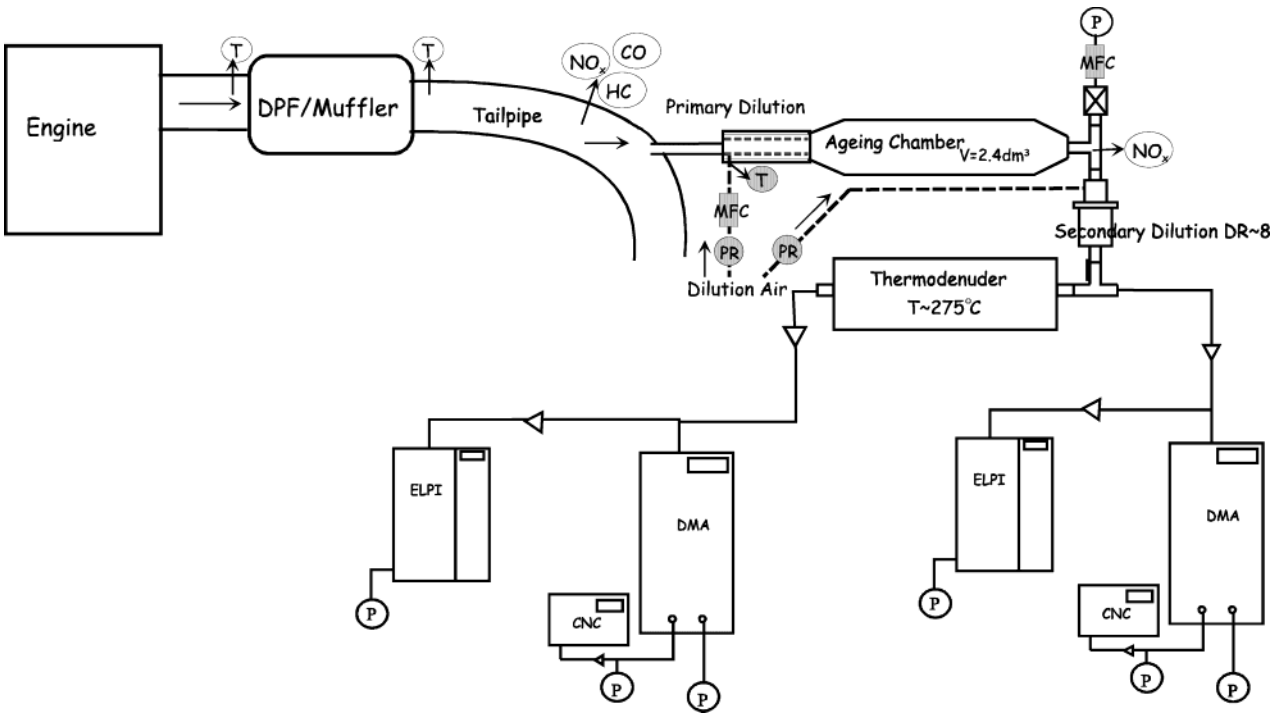

FIGURE 1. Measurement setup.

TABLE 3. Driving Modes

	mode 10	mode 11
speed (rpm)	1800	1800
torque (Nm)	980	245
power (kW)	185	46
load (%)	100	25

a secondary diluter (Figure 1). The flow rate of dilution air was kept constant by another mass flow controller. Dilution ratio was calculated using measured NO_x concentrations in the raw and diluted gas. The temperature of the dilution air in the primary diluter was adjustable (20, 30, and 50 °C were used) and was constantly measured just before the air enters the porous tube. Dilution air could be cooled or heated using a Vortex Tube (model 208BSP-11H, ITW Vortec) or a pressurized air heater (model H42, Dekati, Inc.), respectively.

An ejector with a dilution ratio of 8 was used as a secondary diluter. The pressure of the dilution air was kept constant with a pressure regulator (PR). Particle-free, dry air was used as the dilution air in both diluters. The diluters themselves and the dilution air in the secondary diluter were at ambient temperature. Between the porous tube and the ejector an aging chamber 2.4 dm^3 of volume was added to provide time for the nucleation mode to grow in the counting range of the measurement instruments (see below). Following Ntziachristos et al. (*29*), a residence time in the order of 3 s (2.9 s) was chosen.

The diluted sample was led to measurement instruments both directly and through a thermodenuder (Dekati, Inc.). In this device, sample air is heated to vaporize volatile and semi-volatile part of the particles. The volatile compounds are then absorbed in active charcoal so that they do not recondense onto the remaining solid particles. The temperature in the heating section was set up to 275 °C. The denuder part causes a loss of nonvolatile particles through thermoforetic deposition. The loss is in average 35%, and it was corrected for in all the distribution measurements.

Scanning mobility particle sizer (SMPS, TSI) (*32*) and electrical low-pressure impactor (ELPI, Dekati, Inc.) (*33*) were used to measure the size distribution of the exhaust gas sample. In the measurement setup there were always two pairs of SMPS and ELPI. One pair was placed upstream the thermodenuder, and the other was placed downstream of it. The SMPS was operated at a sheath gas flow of 6 L/min and an aerosol inlet flow of 0.6 L/min, providing a size range of 10−400 nm. In ELPI a filter stage was used providing the size range to begin from approximately 8 nm.

The temperature measurements mentioned above were made by thermocouples. In addition, gaseous emissions (NO_x, CO, HC) in raw exhaust gas were measured with FTIR (Fourier transform infrared spectroscopy).

Results

Measured exhaust gas temperatures, gaseous emissions, and integrated particle number concentrations are presented in Table 4 for modes 10 and 11 with and without CRDPF. The dilution conditions are presented as the dilution ratio (DR) for primary diluter and the temperature of the diluent in the primary diluter (DT). Particulate emissions are presented with the total number concentrations ($1/cm^3$) for nucleation mode and accumulation mode. These values were obtained by fitting size distributions to a log-normal form for nucleation mode and accumulation mode (measured with SMPS) separately. The value for accumulation mode was calculated from the distribution measured after thermodenuder corrected with the losses for solid particles. In some cases, the concentration of either nucleation mode or accumulation mode was too low for reliable total concentration measurement with the dilution ratio used. In those cases, the corresponding value is simply omitted.

Exhaust Gas Temperatures. The temperature of the exhaust slightly decreases in both the CRDPF and the muffler. The main information here is the much higher temperature (∼500 °C) for the high load mode 10 than for mode 11 (∼250 °C).

Gaseous Emissions. Total amounts of carbon monoxide and hydrocarbons are effectively reduced in CRDPF as expected due to the fact that an oxidation catalyst is placed upstream of the filter in the CRDPF (Table 4). The reduction efficiency for both CO and THC is in average near 90%. The

TABLE 4. Emissions from Volvo Engine for Different Configurations

CRDPF (w or w/o)	fuel (S ppm)	*T* (BCRDPF) (°C)	*T* (ACRDPF) (°C)	THC (ppm)	CO (ppm)	NO_x (ppm)	DR	DT (°C)	*N* (nucle) (1/cm³)	*N* (accum) (1/cm³)
Mode 10 (1800 rpm, 980 Nm, 184 kW, 100%)										
w/o	2	514	477	10	86	541	12	30		1.62E+07
							12	50		1.62E+07
							25	20		1.59E+07
	40	502	467	11	74.9	575	12	30		1.68E+07
							12	50		1.61E+07
							25	20		1.63E+07
w	2	522	500	0	12.6	531	12	30	3.42E+06	
							12	50	5.01E+04	
							25	20		
	40	506	492	1	8.4	575	12	30	2.57E+07	
							12	50	2.46E+07	
							25	20	6.32E+05	
Mode 11 (1800 rpm, 245 Nm, 46k W, 25%)										
w/o	2	258	239	39	123	206	12	30	1.84E+07	1.80E+07
							12	50	1.07E+07	1.74E+07
							25	20	6.80E+06	1.96E+07
	40	256	239	35	123	198	12	30	8.01E+06	1.92E+07
							12	50	1.30E+06	1.92E+07
							25	20		1.93E+07
w	2	265	254	7	0.3	206	12	30		
							12	50		
							25	20		
	40	265	257	6	0.7	212	12	30		
							12	50		
							25	20		

CRDPF does not affect the total concentration of NO_x, although the balance between NO and NO_2 probably changes substantially. Between modes 10 and 11 there are clear differences in the concentrations as expected. In mode 10 with higher load, the combustion process is more complete and less HCs and CO are found in the exhaust gas.

Accumulation Mode. With tested fuels and driving modes, the number concentration in accumulation mode is not much affected by either of the fuel or the driving mode (Table 4 and Figure 2). Neither the dilution ratio nor the temperature affects the accumulation mode, but the CRDPF effectively reduces it. Downstream of CRDPF the accumulation mode concentration was too low to be measured reliably with the dilution ratio used. Therefore, no number is given for accumulation mode number in Table 4.

Nucleation Mode. The appearance of nucleation mode is more complex. Without after-treatment, the nucleation mode is formed only at low engine load driving mode 11. No significant difference was found between the fuels (see also Figure 2), indicating that the fuel sulfur level has no effect on this mode, at least not with these low sulfur levels.

The nucleation mode also forms downstream of the CRDPF but now only at the high load mode 10. The effect of fuel is now clearly observable: as the fuel sulfur level gets low enough (to 2 ppm) the nucleation mode is very weak. This can be seen in Figure 2 where the size distributions for different after-treatment configurations, fuels, and driving modes are plotted.

Although not presented here, particle size distribution was recorded in real time with ELPI. The same trends we see from the SMPS results can be observed also from ELPI results. The ELPI was recording before, during, between, and after the SMPS scans were taken so we can be sure that the size distribution remained stable during steady-state driving.

Effect of Dilution Conditions. The tested dilution conditions were found to affect practically the nucleation mode only. With the CRDPF, this is shown in Figure 3 where size distributions measured for different dilution conditions are presented. The nucleation mode gets weaker as the dilution temperature rises or as the dilution ratio increases enough. Similar behavior was observed without the CRDPF.

Effect of Thermodenuder. In all conditions, no nucleation mode was observed with the thermodenuder. The mode therefore consists of semi-volatile compounds that evaporate completely when heated enough (Figure 4). Without CRDPF, the thermodenuder has no observable effect on the accumulation mode in mode 10. This is the case without nucleation mode. To compare the distributions between mode 10 and mode 11 more precisely, these are plotted with linear scale in Figure 4B. The accumulation mode passing through the thermodenuder is practically identical for both driving modes. This means that in both cases the accumulation mode offers equal surface for adsorption and condensation of semi-volatile compounds. However in mode 11 there is significant difference between the accumulation modes with and without the thermodenuder. During the nucleation process, also condensation onto the soot particles obviously takes place, changing the distribution. Because of condensation, accumulation mode becomes narrower, resulting in higher peak concentration. This can be seen from the distribution from which we have subtracted a log-normal fit of the nucleation mode (Figure 4B).

Discussion

The results indicate that two different nucleation modes can be formed with one heavy-duty diesel engine during exhaust gas dilution. One is formed at low load without exhaust gas after-treatment. The other is formed at high load with an oxidation catalyst and filter combination. In Figure 5, we are comparing these two situations. Figure 5A presents the conditions without CRDPF, and Figure 5B presents the conditions with CRDPF. The vertical axis shows both the logarithm of the nucleation mode number concentration and the total hydrocarbon concentration. The horizontal axis is the fuel sulfur level (ppm).

Without CRDPF the nucleation mode is formed only at low engine load. With these low sulfur level fuels, the effect of fuel sulfur on this nucleation mode is not observable. On

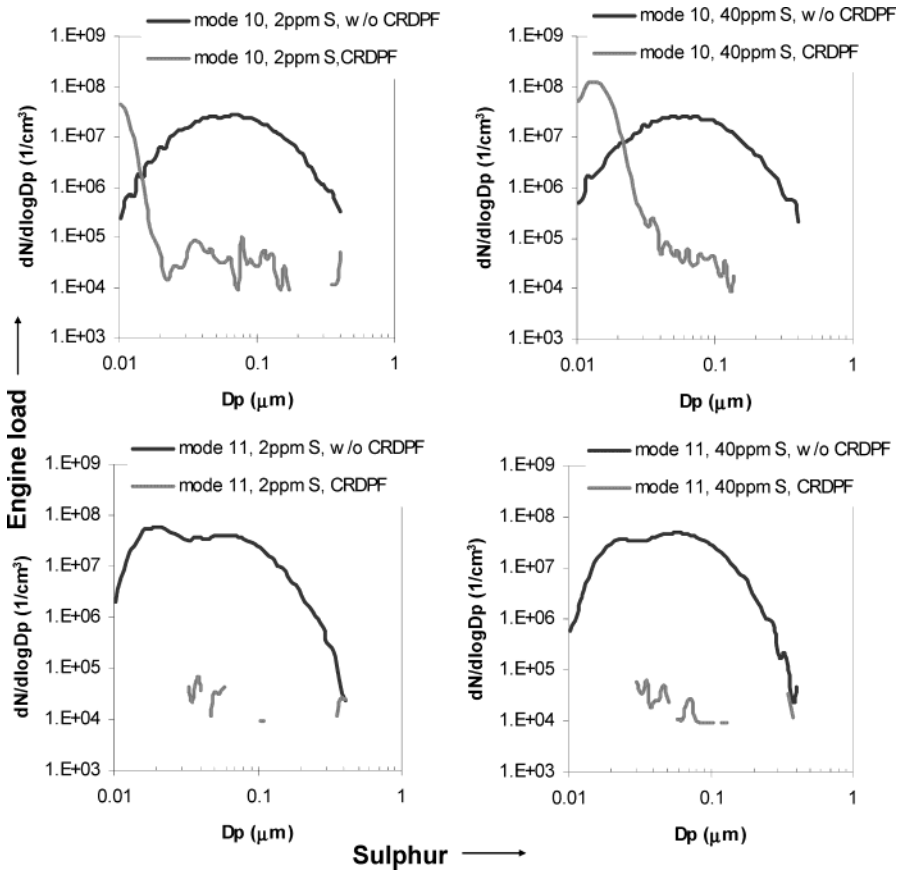

FIGURE 2. Size distributions (measured with SMPS) for different after-treatment configurations and for two fuels in both driving modes with primary dilution ratio being 12 and temperature of 30 °C.

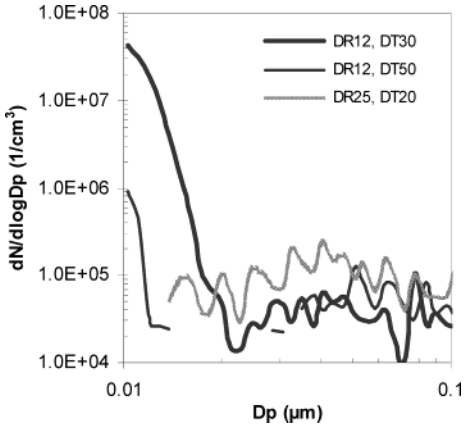

FIGURE 3. Effect of dilution conditions on nucleation mode formed downstream of CRDPF (fuel: 2 ppm S) in mode 10.

the other hand, the hydrocarbon concentration is observed to correlate with the formation of nucleation mode (Figure 5A). For mode 11, with the nucleation mode, the HC emission is several times higher than for mode 10. It is possible that the nucleation mode formation involves nucleation of sulfuric acid and water followed by growth from condensation of organic species, as is suggested to be the case also in studies by Tobias et al. (*15*) and Abdul-Khalek and Kittelson (*6*). The sulfur content of the fuel used by both Tobias et al. (*15*) and Abdul-Khalek and Kittelson (*6*) was near 400 ppm, which is much higher than in the fuels used in this study (2 and 40 ppm). Because of the low sulfur levels in our experiments, the major role of the sulfuric acid and water is not so clear. Anyhow, the major component of the particles is something else, presumably hydrocarbon compound(s).

With the CRDPF, the nucleation mode occurs at high engine load (mode 10). It correlates with the fuel sulfur level (Figure 5B). Although this should be confirmed by further measurements with varying sulfur contents, we believe this correlation is real. Because of the effective oxidation catalyst, the HC concentration is rather low for both modes, and it actually correlates negatively with the formation of nucleation mode. In the Dementhon and Martin (*19*) study, higher load was used for regeneration purposes, and a nucleation peak was observed in the beginning of the regeneration. This was suggested to result from hydrocarbon desorption during regeneration. In our case, the HC concentration was low and stable during the high load drive, accompanied with a stable particle size distribution recorded by ELPI. This is believed to rule out such a process in our case. The circumstantial evidence points to sulfur as a source of nucleation mode downstream of the CRDPF. In CRDPF there are two different components, the oxidation catalyst and the filter, which both can have an effect on the nucleation mode formation. In oxidation catalyst the sulfuric trioxide concentration is increased by catalytic oxidation of sulfuric dioxide. There are two reasons why this oxidation process is expected to be more effective at the high load (mode 10). First, the temperature in the catalyst input is higher in mode 10 (approximately 500 °C) than in mode 11 (approximately 250 °C) favoring the SO_3 formation. Second, due to the higher fuel to air ratio the engine-out SO_2 concentration is also expected to be higher in mode 10 feeding the SO_3 formation more. On the other hand, the lowered adsorption and condensation surface caused by the filtration of the accumulation mode may contribute to the onset of the nucleation process.

Although there are no earlier published studies concerning the formation of nucleation mode with the same kind of

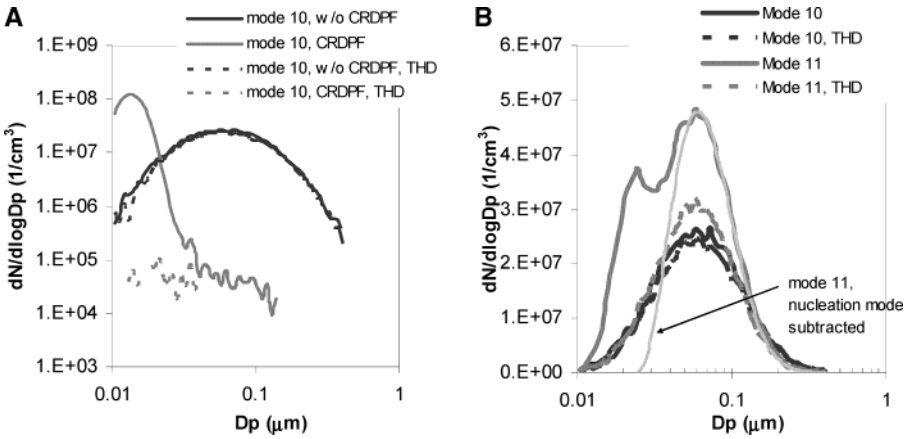

FIGURE 4. (A) Effect of thermodenuder (THD) in mode 10 with and without CRDPF. (B) Comparison of distributions in modes 10 and 11 with and without THD, and distribution in mode 11 from which the nucleation mode has subtracted. Dilution conditions: DR 12, DT 30 °C.

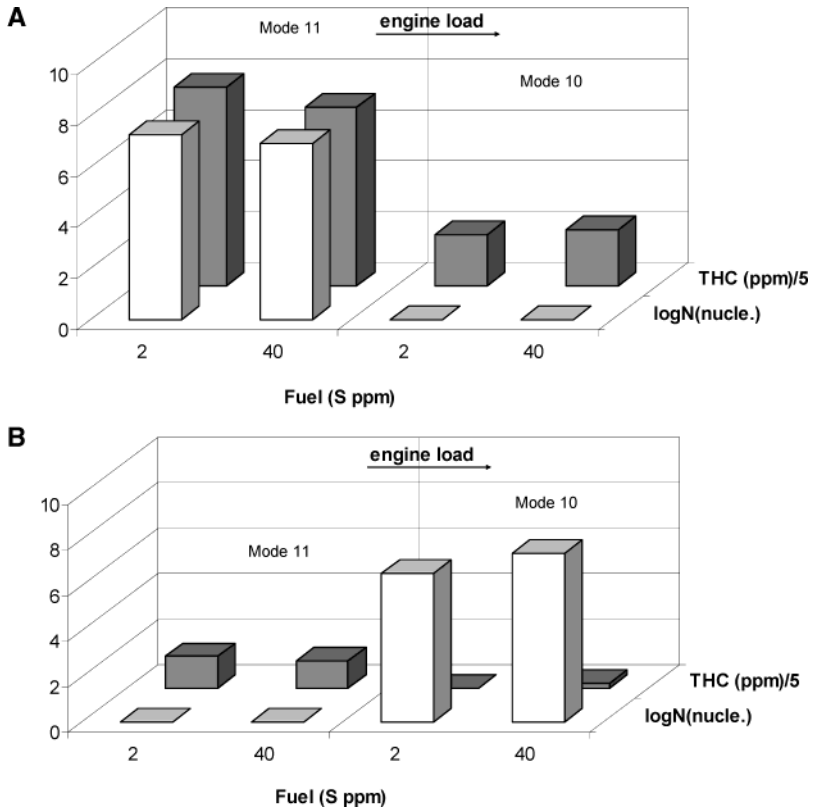

FIGURE 5. Comparison of the logarithm of the number concentration of nucleation mode, the total hydrocarbon concentration (ppm), and the fuel sulfur level (*x*-axis) in both driving modes with CRDPF (A) and without after-treatment (B). Dilution conditions in measurement: DR 12, DT 30 °C.

oxidation catalyst−filter combination used in this study, we believe that these results tie in with those done with other after-treatment systems. The nucleating species are in gaseous phase in the exhaust pipe, at least at the high load modes with high exhaust gas temperatures. The formation of the nucleation mode is believed to take place during cooling and dilution of the exhaust gas. From this point of view, it does not make much difference whether the nucleating compounds are formed in the catalyst, in the filter, or even in the exhaust pipe. With an uncatalyzed filter, Liu et al. (*20*) found the nucleation mode only at high fuel sulfur content. In our study, we still have the nucleation mode with a fuel containing only 2 ppm sulfur. The difference can readily be explained by the use of oxidation catalyst in the CRDPF, which is expected to significantly enhance the SO_3 formation. This is in accordance with the results from Maricq et al. (*22*), as they found the formation of nucleation mode downstream of an oxidation catalyst. In the Lehmann and Mohr (*21*) study, no nucleation mode was observed when placing the oxidation catalyst upstream of the filter. This disagrees with our result but can be attributed to differences in parameters such as the catalyst loadings and gas and catalyst temperatures. Kittelson et al. (*24*) used a catalyzed filter. The present results agree well with their findings. The Hawker et al. (*34*) study also is in good correlation with our result, as they found that sulfates and water emissions were approximately doubled with the kind of CRDPF used in our study.

This study points out the important observation that, for the same engine, nucleation may take place both with a CRDPF and without after-treatment but apparently through

a different mechanism. The nucleation mode formed without CRDPF is suggested to constitute mainly from other components than sulfur, probably hydrocarbons. The nucleation mode formed downstream of an oxidation catalyst−particle filter combination is suggested to form from sulfuric compounds. The trend in near future is further reduction in the fuel sulfur content. Already, there are fuels on the market containing only 1 ppm sulfur. Many after-treatment systems can only efficiently operate with low level sulfur fuels. However, formation of new nanoparticles is possible even with very low sulfur level fuels, as the one used here (2 ppm). When using very low level sulfur fuels, the effect of the sulfur in lubricating oil may become dominating. Reducing this enough may effectively prevent nanoparticle formation related to particle filters.

Acknowledgments

The research was funded by Tekes (National Technology Agency of Finland) and four Finnish companies: Ecocat (formerly Kemira Metalkat), Fortum Oil and Gas, Dekati, and FinnKatalyt. All measurements were done in the engine laboratory of VTT Processes, Engines and Vehicles. We thank the staff of this laboratory, especially Mårten Westerholm. For valuable conversations, we thank Dr. Jyrki Mäkelä.

Literature Cited

(1)) Kittelson, D. *J. Aerosol Sci.* **1998**, *29*, 575−588.
(2) Harrison, R. M.; Jones, M.; Collins, G. *Atmos. Environ.* **1999**, *33*, 309−321.
(3) Shi, J. P.; Evans, D. E.; Khan, A. A.; Harrison, R. M. *Atmos. Environ.* **2001**, *35*, 1193−1202.
(4) Mayer, A.; Czerwinski, J.; Schneidegger, P. *SAE Tech. Pap. Ser.* **1996**, *No. 960472*.
(5) Mayer, A.; Czerwinski, J.; Legerer, F.; Wyser, M. *SAE Tech. Pap. Ser.* **2002**, *No. 2002-01-0435*.
(6) Abdul-Khalek, I.; Kittelson, D.; Brear, F. *SAE Tech. Pap. Ser.* **1998**, *No. 982599*.
(7) Liu, G.; Verdegan, B.; Badeau, K.; Sonsalla, T. *SAE Tech. Pap. Ser.* **2002**, *No. 2002-01-1007*.
(8) Holmen, B. A.; Ayala, A. *Environ. Sci. Technol.* **2002**, *36*, 5041−5050.
(9) Shi, P. I.; Harrison, R. M. *Environ. Sci. Technol.* **1999**, *33*, 3730−3736.
(10) Luders, H.; Kruger, M.; Stommel, P.; Luers, B. *SAE Tech. Pap. Ser.* **1998**, *No. 981374*.
(11) Kittelson, D.; Johnson, J.; Watts, W.; Wei, Q.; Drayton, M.; Paulsen, D.; Bukowiecki, N. *SAE Tech. Pap. Ser.* **2000**, *No. 2000-01-2212*.
(12) Vehkamäki, H.; Kulmala, M.; Lehtinen, K. E. J.; Noppel, M. *Environ. Sci. Technol.* **2003**, *37*, 3392−3398.
(13) Saito, K.; Shinozaki, O.; Seto, T.; Kim, C.-S.; Okuyama, K.; Kwon, S.-B.; Lee, K. W. *SAE Tech. Pap. Ser.* **2002**, *No. 2002-01-1008*.
(14) Khalek, I. A.; Spears, M.; Charmley, W. *SAE Tech. Pap. Ser.* **2003**, *No. 2003-01-0285*.
(15) Tobias, H. J.; Beving, D. E.; Ziemann, P. J.; Sakurai, H.; Zuk, M.; McMurry, P. H.; Zarling, D.; Waytulonis, R.; Kittelson, D. B. *Environ. Sci. Technol.* **2001**, *35*, 2233−2243.
(16) Yu, F. *Geophys. Res. Lett.* **2001**, *28*, 4191−4194.
(17) Yu, F. *Geophys. Res. Lett.* **2002**, *29*, No.15.
(18) Kittelson, D. B. Recent measurements of nanoparticle emissions from engines. Presented at the Meeting on Current Research on Diesel Exhaust Particles, Japan Association of Aerosol Science and Technology, January 2001, Tokyo, Japan.
(19) Dementhon, J.-B.; Martin B. *SAE Tech. Pap. Ser.* **1997**, *No. 972999*.
(20) Liu, Z. G.; Skemp, M. D.; Lincoln, J. C. *SAE Tech. Pap. Ser.* **2003**, *No. 2003-01-0046*.
(21) Lehmann, U.; Mohr, M. *Int. J. Vehicle Des.* **2001**, *27* (1−4), 228−241.
(22) Maricq, M.; Chase, R.; Xu, N.; Laing, P. *Environ. Sci. Technol.* **2002**, *36*, 283−289.
(23) Vogt, R.; Scheer, V.; Casati, R.; Benter, T. *Environ. Sci. Technol.* **2003**, *37*, 4070−4076.
(24) Kittelson, D.; Watts, W.; Johnson, J. *Diesel Aerosol Sampling Methodology—CRC E-43*; Final report; University of Minnesota, Department of Mechanical Engineering: Minneapolis, MN, 2002 (www.crcao.com).
(25) Wåhlin, P.; Palmgren, F.; Van Dingenen, R. *Atmos. Environ.* **2001**, *35*, S63−S69.
(26) Charron, A.; Harrison, R. M. *Atmos. Environ.* **2003**, *37*, 4109−4119.
(27) Abu-Allaban, M.; Coulomb, W.; Gertler, A. W.; Gillies, J.; Pierson, W. R.; Rogers, C. F.; Sagebiel, J. C.; Tarnay, L. *Aerosol Sci. Technol.* **2002**, *36*, 771−789.
(28) Gidhagen, L.; Johansson, C.; Ström, J.; Kristensson, A.; Swietlicki, E.; Pirjola, L.; Hansson, H.-C. *Atmos Environ.* **2003**, *37*, 2023−2036.
(29) Ntziachristos, L.; Giechaskiel, B.; Pistikopoulos, P.; Samaras, Z.; Mathis, U.; Mohr, M.; Ristimäki, J.; Keskinen, J.; Mikkanen, P.; Casati, R.; Scheer, V.; Vogt, R. *SAE Tech. Pap. Ser.* **2004**, *No. 2004-01-1439*.
(30) Cooper, B. J.; Jung, H. J.; Thoss, J. E. U.S. Patent No. 4,902,487, 1988.
(31) Mikkanen, P.; Moisio, M.; Keskinen, J.; Ristimäki, J.; Marjamäki, M. *SAE Tech. Pap. Ser.* **2001**, *No. 2001-01-0219*.
(32) Wang, S. C.; Flagan, R. C. *Aerosol Sci. Technol.* **1990**, *13*, 230−240.
(33) Keskinen, J.; Pietarinen, K.; Lehtimäki, M. *J. Aerosol Sci.* **1992**, *23*, 353−360.
(34) Hawker, P.; Huthwolh, G.; Henn, J.; Koch, W.; Luders, H.; Luders, B.; Stommel, P. *SAE Tech. Pap. Ser.* **1998**, *No. 980189*.

Received for review November 28, 2003. Revised manuscript received June 24, 2004. Accepted June 24, 2004.

ES0353255